Journal of Biomolecular NMR, **11:** 213–220, 1998.
KLUWER/ESCOM

A sensitive pulse scheme for measuring the backbone dihedral angle ψ based on cross-correlation between $^{13}C^{\alpha}$-$^{1}H^{\alpha}$ dipolar and carbonyl chemical shift anisotropy relaxation interactions

Daiwen Yang, Kevin H. Gardner and Lewis E. Kay
Protein Engineering Network Centers of Excellence and Departments of Molecular and Medical Genetics, Biochemistry and Chemistry, University of Toronto, Toronto, ON, Canada M5S 1A8

Received 7 November 1997; Accepted 5 December 1997

Key words: chemical shift anisotropy, cross-correlation, psi

Abstract

A pulse scheme for measuring cross-correlation between $^{13}C^{\alpha}$-$^{1}H^{\alpha}$ dipolar and carbonyl chemical shift anisotropy relaxation mechanisms is presented from which the protein backbone dihedral angle ψ is measured. The method offers significant sensitivity gains relative to our recently published scheme for measuring ψ based on this cross-correlation effect [Yang et al. (1997) *J. Am. Chem. Soc.*, **119**, 11938–11940]. The utility of the method is demonstrated with an application to a 42 kDa complex of ^{15}N,^{13}C-labeled maltose binding protein and β-cyclodextrin.

Pioneering studies, largely by Grant, Werbelow and co-workers, have established that cross-correlated spin relaxation can provide a detailed understanding of molecular dynamics in solution (Werbelow and Grant, 1977). Recently, Griesinger and co-workers have shown that it is possible to use cross-correlated spin relaxation to obtain information about molecular structure as well (Reif et al., 1997). In their elegant experiment, cross-correlated relaxation between $^{13}C^{\alpha}$-$^{1}H^{\alpha}$ and ^{15}N-NH dipolar fields was used to measure the backbone dihedral angle ψ in the protein rhodniin. We have recently developed a similar experiment based on the measurement of cross-correlated relaxation between $^{13}C^{\alpha}$-$^{1}H^{\alpha}$ dipolar and carbonyl ($^{13}C'$) chemical shift anisotropy (CSA) relaxation mechanisms for the measurement of ψ that enjoys sensitivity advantages over the dipole–dipole cross-correlation experiment (Yang et al., 1997). Excellent agreement between experimentally measured cross-correlated relaxation rates and rates calculated theoretically on the basis of X-ray derived structures of a number of proteins [ubiquitin (Vijay-Kumar et al., 1987) and CheY (Stock et al., 1994)] was obtained. Nevertheless, a potential limitation of the experiment lies in the use of a fixed delay during which cross-correlated relaxation evolves which must be set to the inverse of J_{CC} (the one-bond aliphatic ^{13}C-^{13}C coupling). This delay, required to minimize net evolution and hence sensitivity losses resulting from homonuclear ^{13}C-^{13}C scalar coupling effects, is often longer than optimal for applications to large proteins, resulting in spectra with a poor signal to noise ratio. With this problem in mind we have developed an experiment which improves the sensitivity of our original scheme. We illustrate the utility of the new approach by measuring cross-correlated relaxation rates in a complex of β-cyclodextrin and ^{15}N,^{13}C-labeled maltose binding protein (42 kDa).

At the core of our original $^{13}C^{\alpha}$-$^{1}H^{\alpha}$ dipolar/$^{13}C'$ CSA experiment is the generation of double- and zero-quantum $^{13}C'$-$^{13}C^{\alpha}$ coherences which are allowed to evolve for a fixed period, of duration T_C, during which relaxation occurs. In this interval evolution also proceeds due to the one-bond $^{13}C^{\alpha}$-$^{1}H^{\alpha}$ scalar coupling, J_{CH}, so that cross peaks are observed at frequencies $\omega_{C'} + \omega_{C\alpha} \pm \pi J_{CH}$ in the case of double-quantum spectra and at $-\omega_{C'} + \omega_{C\alpha} \pm \pi J_{CH}$ in zero-quantum data sets. The transverse relaxation rates of each of the double- and zero-quantum multiplet components can

be calculated by considering an $^1H^\alpha$-$^{13}C^\alpha$-$^{13}C'$ spin system. It can be shown that the relaxation rates are given by

$$\begin{aligned}\Gamma_{2Q,\alpha} &= \Gamma_a + \Gamma_{H\alpha C\alpha,C\alpha} + \Gamma_{H\alpha C\alpha,C'} + \Gamma_{C\alpha C'}\\ \Gamma_{2Q,\beta} &= \Gamma_a - \Gamma_{H\alpha C\alpha,C\alpha} - \Gamma_{H\alpha C\alpha,C'} + \Gamma_{C\alpha C'}\\ \Gamma_{0Q,\alpha} &= \Gamma_a + \Gamma_{H\alpha C\alpha,C\alpha} - \Gamma_{H\alpha C\alpha,C'} - \Gamma_{C\alpha C'}\\ \Gamma_{0Q,\beta} &= \Gamma_a - \Gamma_{H\alpha C\alpha,C\alpha} + \Gamma_{H\alpha C\alpha,C'} - \Gamma_{C\alpha C'}\end{aligned} \quad (1)$$

where $\Gamma_{aQ,g}$ is the relaxation rate of the a-quantum ($a = 0, 2$) $^{13}C'$-$^{13}C^\alpha$ coherence, g is the spin state ($g = \alpha, \beta$) of the $^1H^\alpha$ proton, Γ_a is the auto-relaxation rate of each of the lines, $\Gamma_{H\alpha C\alpha,C\alpha}$ ($\Gamma_{H\alpha C\alpha,C'}$) is the cross-correlation relaxation rate derived from the $^{13}C^\alpha$-$^1H^\alpha$ dipolar/$^{13}C^\alpha$ ($^{13}C'$) CSA interactions and $\Gamma_{C\alpha C'}$ is the rate arising from cross-correlated relaxation between $^{13}C^\alpha$ and $^{13}C'$ CSA terms. It is worth noting that contributions to relaxation from neighboring protons will affect all lines equally (increase in Γ_a). As we showed previously (Yang et al., 1997), by measuring the intensities of each of the components in $^{13}C'$-$^{13}C^\alpha$ double- and zero-quantum spectra it is possible to obtain the cross-correlation relaxation rate for the $^{13}C^\alpha$-$^1H^\alpha$ dipolar/$^{13}C'$ CSA interaction according to

$$\Gamma_{H\alpha C\alpha,C'} = (0.25/T_C)\ln[(I_{2Q,\beta}I_{0Q,\alpha})/(I_{2Q,\alpha}I_{0Q,\beta})] \quad (2)$$

where $I_{aQ,g}$ is the intensity of the a-quantum $^{13}C'$-$^{13}C^\alpha$ component coupled to a $^1H^\alpha$ proton of spin state g. The value of $\Gamma_{H\alpha C\alpha,C'}$ can be directly related to the dihedral angle ψ according to Equations (1) and (2) of Yang et al. (1997) (see below). A more complete calculation shows that contributions from the cross-correlation between $^{13}C'$-$^1H^\alpha$ dipolar and $^{13}C^\alpha$ CSA interactions cannot be separated from the $^{13}C^\alpha$-$^1H^\alpha$ dipolar/$^{13}C'$ CSA term; the former effect is, however, much smaller, as we have discussed previously (Yang et al., 1997).

At first glance, Equation (2) seems to indicate that the intensities of both double- and zero-quantum $^{13}C'$-$^{13}C^\alpha$ components are required to obtain $\Gamma_{H\alpha C\alpha,C'}$ and indeed our original scheme was based on recording all four multiplet components. However, because the intensity of a component, $I_{aQ,g}$, is simply given by

$$I_{aQ,g} = \exp(-\Gamma_{aQ,g}T_C) \quad (3)$$

it follows that Equation (2) can be rewritten as

$$\Gamma_{H\alpha C\alpha,C'} = (1/2)\{1/2[\Gamma_{2Q,\alpha} + \Gamma_{0Q,\beta}] - 1/2[\Gamma_{2Q,\beta} + \Gamma_{0Q,\alpha}]\} \quad (4)$$

Thus, it is sufficient to measure the average relaxation rates of the 2Q,α and 0Q,β components (frequencies of $\omega_{C'} \pm \omega_{C\alpha} - \pi J_{CH}$, denominator of Equation (2)) and, correspondingly, the average rates of 2Q,β and 0Q,α components (frequencies of $\omega_{C'} \pm \omega_{C\alpha} + \pi J_{CH}$, numerator of Equation (2)). Therefore, if the 2Q,α and 0Q,β components are interchanged midway through the period T_C, with interchange of 0Q,α and 2Q,β multiplets as well, a simplified spectrum results (see below) in which the averages indicated in Equation (4) are generated *de facto* during the course of the pulse scheme. Recall that the 2Q,α and 0Q,β components are derived from the transitions, $\alpha\beta\beta \rightarrow \alpha\alpha\alpha$ and $\beta\alpha\beta \rightarrow \beta\beta\alpha$, where the three spin functions from left to right correspond to $^1H^\alpha$,$^{13}C^\alpha$ and $^{13}C'$ states [0Q,α and 2Q,β are derived from $\alpha\alpha\beta \rightarrow \alpha\beta\alpha$ and $\beta\beta\beta \rightarrow \beta\alpha\alpha$, respectively]. Thus, the interchange of components can be readily accomplished by the simultaneous (or successive in our case, see below) application of $^1H^\alpha$ and $^{13}C^\alpha$ 180° pulses at the midpoint of the T_C period.

Figure 1 illustrates the pulse scheme that we have developed to measure $\Gamma_{H\alpha C\alpha,C'}$ with increased sensitivity. As with the previous sequence for measuring $^{13}C^\alpha$-$^1H^\alpha$ dipolar/$^{13}C'$ CSA interactions, the scheme is based on an HNCOCA magnetization transfer (Bax and Ikura, 1991). At point a in the sequence double- and zero-quantum $^{13}C'$-$^{13}C^\alpha$ coherences are generated and allowed to evolve for the period A+B+C+D illustrated in Figure 1. During this complete period cross-correlated relaxation resulting from $^{13}C^\alpha$-$^1H^\alpha$ dipolar/$^{13}C'$ CSA relaxation mechanisms is operative. In this regard, the application of $^{13}C^\alpha$ 180° pulses (three shaped pulses between a and b in Figure 1) is accompanied by either $^{13}C'$ or ^1H (not both) 180° pulses. Note that the terms which contribute to the $^{13}C'$ CSA and $^{13}C^\alpha$-$^1H^\alpha$ dipolar Hamiltonians, $\mathcal{H}_1$ and $\mathcal{H}_2$, respectively, in the macromolecular limit can be written as (Abragam, 1961)

$$\begin{aligned}\mathcal{H}_1 &\propto C'_Z\\ \mathcal{H}_2 &\propto C^\alpha_Z I_Z\end{aligned} \quad (5)$$

where C'_Z , C^α_Z and I_Z are the z-spin angular momentum operators for $^{13}C'$, $^{13}C^\alpha$ and $^1H^\alpha$ spins. Therefore, the successive application of $^{13}C^\alpha$ and $^1H^\alpha$ 180° pulses or $^{13}C^\alpha$ and $^{13}C'$ 180° pulses preserves the relative signs of the Hamiltonians in Equation (5) and hence ensures that the terms resulting from evolution due to cross-correlation between $\mathcal{H}_1$ and $\mathcal{H}_2$ both prior to and after the application of the pulses will add constructively. It is important to recognize that the $^{13}C'$

and $^{13}C^{\alpha}$ pulses are applied successively ($^{13}C^{\alpha}$ before $^{13}C'$) and not simultaneously, since the large field which is employed for the $^{13}C^{\alpha}$ pulses would interfere with the effects of the $^{13}C'$ pulses. A second point of interest is that the $^{13}C^{\alpha}$ 180° pulse of phase $\phi 4$ (between B and C) is selective and intended to refocus $^{13}C^{\alpha}$ magnetization without inverting $^{13}C^{\beta}$ spins. In this way the evolution of $^{13}C^{\alpha}$ magnetization during the delay $A + B (= T_C/2)$ resulting from J_{CC} is refocused during the subsequent delay $C + D (= T_C/2)$; note that the two $^{13}C^{\alpha}$ refocusing pulses between A and B and C and D are non-selective [400 μs RE-BURP (Geen and Freeman, 1991) pulses]. Therefore, the constant time period between a and b can be of any duration, rather than a multiple of $1/J_{CC}$ which might otherwise be selected so that $^{13}C^{\alpha}$-$^{13}C^{\beta}$ scalar couplings would not decrease the sensitivity of the experiment. The selectivity of this $^{13}C^{\alpha}$ pulse dictates that its duration be significant (2 ms RE-BURP). Thus, the simultaneous application of $^{13}C^{\alpha}$ and $^{1}H^{\alpha}$ 180° pulses would result in a substantial loss in sensitivity from $^{1}H^{\alpha}$-$^{13}C^{\alpha}$ J-evolution which would occur during the application of the $^{13}C^{\alpha}$ pulse. This unacceptable loss in signal is easily avoided by applying the pulses successively.

Unlike the previous pulse sequence for measuring $\Gamma_{H\alpha C\alpha,C'}$, where sums and differences of $^{13}C^{\alpha}$ and $^{13}C'$ shifts are recorded during t_1, $^{13}C^{\alpha}$ chemical shift evolution between points a and b is refocused in the scheme of Figure 1 so that only the $^{13}C'$ chemical shift is recorded during this period. This can be understood by recalling that the 2Q,α and 0Q,β lines resonate with frequencies of $\omega_{C'} + \omega_{C\alpha} - \pi J_{CH}$ and $\omega_{C'} - \omega_{C\alpha} - \pi J_{CH}$, while the 0Q,α and 2Q,β components are at frequencies of $\omega_{C'} - \omega_{C\alpha} + \pi J_{CH}$ and $\omega_{C'} + \omega_{C\alpha} + \pi J_{CH}$, respectively. Therefore, we can write

$$\begin{aligned}
&\rho_{2Q,\alpha}(T_C) = \\
&\rho_{0Q,\beta}(T_C) \propto \exp(-i\omega_{0Q,\beta}t_1/2)\exp(-\Gamma_{0Q,\beta}T_C/2)\times \\
&\qquad \exp(-i\omega_{2Q,\alpha}t_1/2)\exp(-\Gamma_{2Q,\alpha}T_C/2) \\
&\qquad = \exp[-i(\omega_{C'} - \pi J_{CH})t_1]\times \\
&\qquad \exp[-0.5(\Gamma_{0Q,\beta} + \Gamma_{2Q,\alpha})T_C] \\
&\rho_{0Q,\alpha}(T_C) = \\
&\rho_{2Q,\beta}(T_C) \propto \exp(-i\omega_{2Q,\beta}t_1/2)\exp(-\Gamma_{2Q,\beta}T_C/2)\times \\
&\qquad \exp(-i\omega_{0Q,\alpha}t_1/2)\exp(-\Gamma_{0Q,\alpha}T_C/2) \\
&\qquad = \exp[-i(\omega_{C'} + \pi J_{CH})t_1]\times \\
&\qquad \exp[-0.5(\Gamma_{2Q,\beta} + \Gamma_{0Q,\alpha})T_C] \qquad (6)
\end{aligned}$$

where the density matrix element $\rho_{aQ,g}(T_C)$ is the value at the end of the constant time period of duration T_C, immediately prior to the application of the $^{13}C^{\alpha}$ 90° pulse of phase $\phi 5$ at point b in Figure 1. An analogous situation occurs in the 2D ^{1}H-X HMQC experiment (Mueller, 1979; Bax et al., 1983), where despite the fact that both ^{1}H and X zero- and double-quantum coherences are present during t_1, ^{1}H chemical shift is refocused, resulting in a data set in which only the X chemical shift is recorded in t_1. In the present experiment, spectra are obtained with cross peaks at $(\omega_{C'}[i] \pm \pi J_{CH}, \omega_N[i+1], \omega_{NH}[i+1])$ where i and $i + 1$ emphasize that the correlation connects the C′ of residue i with the amide shifts of residue $i + 1$. Thus, spectra are more readily analyzed relative to data sets where zero- and double-quantum frequencies are measured since (i) an HNCO-type data set is generated and (ii) $\Gamma_{H\alpha C\alpha,C'}$ is obtained from the relative intensities of two multiplet components (rather than four) resonating at $\omega_{C'} \pm \pi J_{CH}$, as discussed below.

From Equations (1) and (6) it follows directly that the relaxation rates of the two F_1-multiplet components generated by the scheme of Figure 1 are given by

$$\begin{aligned}
&\Gamma_{2Q,\alpha+0Q,\beta} = \Gamma_a + \Gamma_{H\alpha C\alpha,C'} \\
&\Gamma_{2Q,\beta+0Q,\alpha} = \Gamma_a - \Gamma_{H\alpha C\alpha,C'} \qquad (7)
\end{aligned}$$

where $\Gamma_{2Q,\alpha+0Q,\beta}$ is the average relaxation rate of the component with an ω_1 frequency of $\omega_{C'} - \pi J_{CH}$, $(\omega_{C'} > 0)$ corresponding to the interchange of transitions $\alpha\beta\beta \rightarrow \alpha\alpha\alpha$ and $\beta\alpha\beta \rightarrow \beta\beta\alpha$ in the center of the constant time period (between a and b in Figure 1), while $\Gamma_{2Q,\beta+0Q,\alpha}$ is the average relaxation rate of the multiplet at $\omega_{C'} + \pi J_{CH}$, derived from the interchange of transitions $\beta\beta\beta \rightarrow \beta\alpha\alpha$ and $\alpha\alpha\beta \rightarrow \alpha\beta\alpha$. From Equation (7) we can write

$$\begin{aligned}
&\Gamma_{H\alpha C\alpha,C'} = \\
&(0.5/T_C)\ln[(I_{2Q,\beta+0Q,\alpha})/(I_{2Q,\alpha+0Q,\beta})] \qquad (8)
\end{aligned}$$

where $I_{2Q,\beta+0Q,\alpha}$ and $I_{2Q,\alpha+0Q,\beta}$ are the intensities of the doublet components at $\omega_{C'} + \pi J_{CH}$ and $\omega_{C'} - \pi J_{CH}$, respectively, and from which Equation (4) follows directly. As described previously (Yang et al., 1997), $\Gamma_{H\alpha C\alpha,C'}$ can be recast according to

$$\begin{aligned}
&\Gamma_{H\alpha C\alpha,C'} = \\
&(4/15)(h/2\pi)\omega_C\gamma_C\gamma_H r_{HC}^{-3}\tau_C f(\sigma_X, \sigma_Y, \sigma_Z) \qquad (9.1)
\end{aligned}$$

where

$$\begin{aligned}
&f(\sigma_X, \sigma_Y, \sigma_Z) = 0.5[\sigma_X(3\cos^2\theta_X - 1) + \\
&\sigma_Y(3\cos^2\theta_Y - 1) + \sigma_Z(3\cos^2\theta_Z - 1)] \qquad (9.2)
\end{aligned}$$

γ_i is the gyromagnetic ratio of spin i, r_{HC} is the distance between $^{1}H^{\alpha}$ and $^{13}C^{\alpha}$ nuclei, τ_c is the correlation time describing the overall tumbling of the

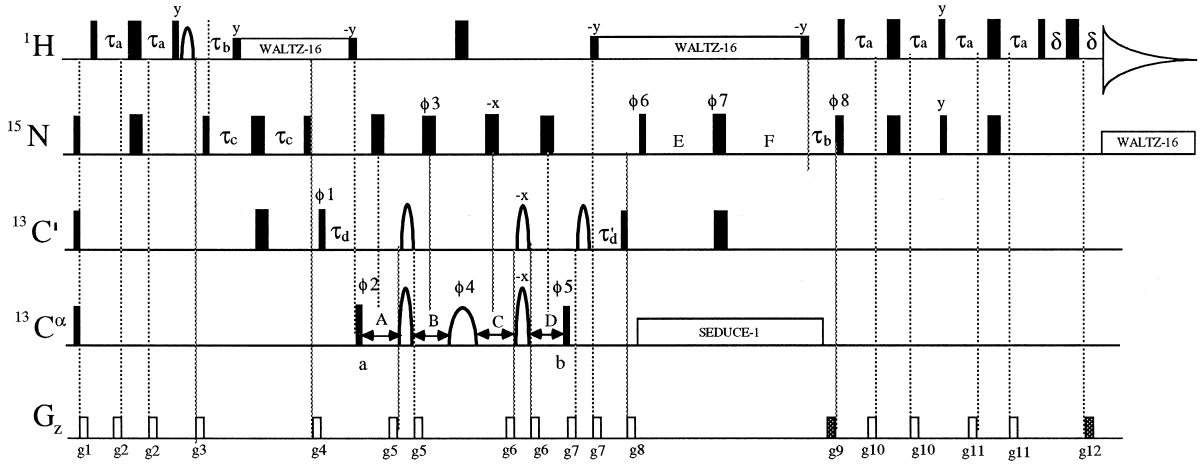

Figure 1. Pulse scheme used to measure cross-correlation between $^{13}C^{\alpha}$-$^{1}H^{\alpha}$ dipolar and carbonyl chemical shift anisotropy relaxation mechanisms. All narrow (wide) pulses are applied with flip angles of 90° (180°) and are along the x-axis, unless indicated otherwise. The ^{1}H, ^{13}C and ^{15}N carriers are positioned at 4.72 ppm (water), 176 ppm and 119 ppm. All proton pulses are applied with a 22 kHz field with the exception of the WALTZ decoupling elements (Shaka et al., 1983) and the flanking pulses (6 kHz). ^{15}N pulses use a 6.2 kHz field, with WALTZ-16 decoupling achieved with a 1 kHz field. All $^{13}C'$ and $^{13}C^{\alpha}$ rectangular pulses are applied with a field strength of $\Delta/\sqrt{15}$, where Δ is the separation in Hz between the centers of the $^{13}C^{\alpha}$ and $^{13}C'$ spectral regions (Kay et al., 1990). The $^{13}C'$ shaped pulses have r-SNOB profiles (390 μs, 6.0 kHz peak rf) (Kupce et al., 1995) while the $^{13}C^{\alpha}$ shaped pulses make use of RE-BURP profiles (Geen and Freeman, 1991). The non-selective refocusing $^{13}C^{\alpha}$ pulses (first and third shaped pulses) are 400 μs (15.5 kHz peak rf, excitation centered at 50 ppm), while the $^{13}C^{\alpha}$ selective refocusing pulse (phase ϕ4) is of duration 2 ms (3.2 kHz peak rf, excitation centered at 55 ppm). The phase of the selective $^{13}C^{\alpha}$ pulse is adjusted carefully to ensure optimal sensitivity. Note that the $^{13}C'$ and $^{13}C^{\alpha}$ refocusing pulses are not applied simultaneously. Rather, the higher power $^{13}C^{\alpha}$ pulses are applied prior to the $^{13}C'$ pulses in both cases, compensating the Bloch–Siegert effects on the $^{13}C'$ magnetization (Vuister and Bax, 1992). The ^{1}H 180° pulse between B and C is applied prior to the 2 ms $^{13}C^{\alpha}$ pulse. $^{13}C^{\alpha}$ decoupling during the ^{15}N evolution period is achieved using WALTZ-16 with the shape of each of the elements (355.5 μs) given by the SEDUCE-1 profile (McCoy and Mueller, 1992). The delays used are: $\tau_a = 2.3$ ms; $\tau_b = 5.3$ ms; $\tau_c = 12.4$ ms; $\tau_d = 8.6$ ms + pwsel/2, where pwsel is the selective $^{13}C^{\alpha}$ refocusing pulse (2 ms); $\tau'_d = 8.6$ ms – pwsel/2; $\delta = 0.5$ ms; $A = (T_C + t_1)/4$; $B = (T_C - t_1)/4$; $C = (T_C - t_1)/4$; $D = (T_C + t_1)/4$; $E = T_N - t_2/2$; $F = T_N + t_2/2 - \tau_b$; $T_c = 28$ ms for ubiquitin, 18 ms for CheY and 10.4 ms for maltose binding protein; $T_N = 12.4$ ms. The phase cycling employed is: $\phi_1 = -x, 2(x), -x$; $\phi_2 = y, -y$; $\phi_3 = x, -x$; $\phi_4 = 8(x), 8(y), 8(-x), 8(-y)$; $\phi_5 = 4(y), 4(-y)$; $\phi_6 = x$; $\phi_7 = 4(x), 4(-x)$; $\phi_8 = x$; rec = $2(x), 4(-x), 2(x), 2(-x), 4(x), 2(-x)$. Quadrature detection in F_1 is achieved by States-TPPI of ϕ_1 (Marion et al., 1989) while quadrature in F_2 employs the enhanced sensitivity pulsed field gradient method (Kay et al., 1992; Schleucher et al., 1993), where for each value of t_2 separate data sets are recorded for (g9, ϕ_8) and ($-$g9, $\phi_8 + 180°$). For each successive t_2 value, ϕ_6 and the phase of the receiver are incremented by 180°. The duration and strengths of the gradients are: g1=(0.5 ms, 8 G/cm); g2 = (0.5 ms, 5 G/cm); g3 = (1 ms, $-$15 G/cm); g4 = (1 ms, 10 G/cm); g5 = (0.1 ms, $-$20 G/cm); g6 = (0.4 ms, 20 G/cm); g7 = (0.3 ms, 5 G/cm); g8 = (1 ms, 15 G/cm); g9 = (1.25 ms, 30 G/cm); g10 = (0.4 ms, 5 G/cm); g11 = (0.3 ms, 4 G/cm); g12 = (0.125 ms, 29 G/cm). Decoupling is interrupted prior to the application of gradients (Kay, 1993). It is important that all delays and pulses be properly accounted for. Copies of the pulse programming code are available upon request.

assumed rigid and isotropically tumbling molecule, ω_C is the carbon Larmor frequency, σ_i is the ith principal component of the chemical shift tensor (values given in the legend to Figure 2) and $\cos\theta_i$ is the direction cosine defining the orientation of the $^{13}C^{\alpha}$-$^{1}H^{\alpha}$ bond with respect to the i axis of the carbonyl shift tensor (Goldman, 1984). Finally, the direction cosines can be recast in terms of the dihedral angle ψ according to

$$\begin{aligned}\cos\theta_X &= -0.3095 + 0.3531\cos(\psi - 120°)\\ \cos\theta_Y &= -0.1250 - 0.8740\cos(\psi - 120°)\\ \cos\theta_Z &= -0.9426\sin(\psi - 120°)\end{aligned} \qquad (10)$$

for non-glycine residues. In the case of glycine, $\Gamma_{H\alpha C\alpha,C'}$ can be obtained by using the intensities of only the most upfield and most downfield components of the triplet in Equation (8) and substituting $f(\sigma_X, \sigma_Y, \sigma_Z)$ with $f_1(\sigma_X, \sigma_Y, \sigma_Z) + f_2(\sigma_X, \sigma_Y, \sigma_Z)$, where $f_1 = f$ and f_2 is obtained by replacing $(\psi - 120°)$ with $(\psi + 120°)$ in Equation (10) (Yang et al., 1997). On a practical note regarding the use of Equations (8–10) to extract ψ, $rmI_{2Q,\alpha+0Q,\beta}$ and $I_{2Q,\beta+0Q,\alpha}$ (see Equation (8)) correspond to the intensities of the upfield and downfield components in spectra recorded with the scheme of Figure 1, respectively. Note that in Equation (2) $I_{qQ,\alpha}$ and $I_{qQ,\beta}$ are the intensities of the upfield and downfield components in $^{13}C^{\alpha}$-$^{13}C'$ q-quantum spectra (q = 0, 2).

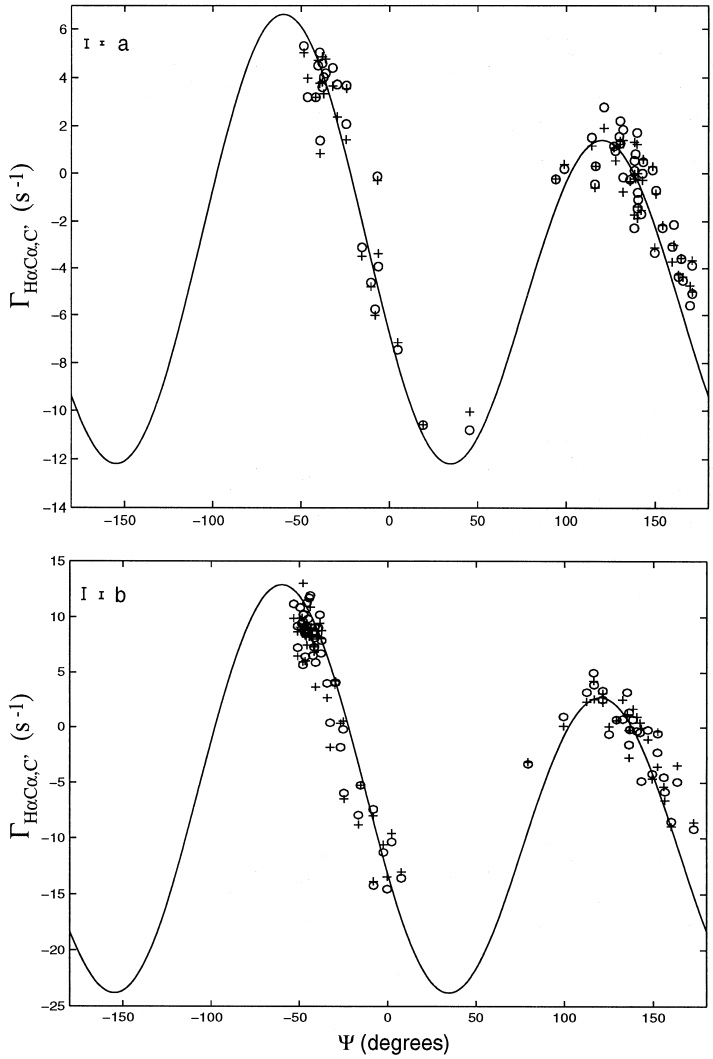

Figure 2. Correlation between calculated (solid) and experimental values of $\Gamma_{H\alpha C\alpha,C'}$ and ψ for non-glycine residues in ubiquitin (a) and CheY (b) obtained from the previously published method of Yang et al. (1997) [+] and the present scheme [○]. Average errors obtained with the two methods are shown by the vertical bars in the upper left hand corner, with the smaller bar corresponding to the results from the method of Figure 1. A 2 mM ubiquitin sample, 50 mM potassium phosphate, pH 5.0, 30 °C was employed and a total measuring time of 19 h was used to record the 3D data set using the scheme described herein with $T_C = 28$ms [$28 \times 18 \times 512$ complex points with acquisition times of 23.2, 17.8 and 64 ms in (t_1,t_2,t_3)]. In the case of CheY (1.8 mM, 5 mM $MgCl_2$, 0.1 M phosphate buffer, pH 6.8, 30 °C) a data set was recorded in 36 h [$36 \times 24 \times 512$ complex points with acquisition times of 15.1, 23.7 and 64 ms in (t_1,t_2,t_3), $T_C = 18$ ms]. Values of (244, 178, 90 ppm) were used for (σ_X, σ_Y, σ_Z) (Teng et al., 1992). All spectra were recorded on a Varian Unity+ 500 MHz spectrometer with data processing and analysis achieved using the programs NMRPipe (Delaglio et al., 1995) and PIPP/CAPP (Garrett et al., 1991), respectively. Values for $\Gamma_{H\alpha C\alpha,C'}$ were obtained from Equation (8) with the intensities of the downfield and upfield multiplet components in F_1 used for the numerator and denominator, respectively. Note that, depending on how the sequence is coded, the net time that cross-correlation evolves may differ slightly from T_C. In our case the $^{13}C^{\alpha}$ shaped pulses between A and B and between C and D were applied prior to the $^{13}C'$ pulses and the durations of the $^{13}C'$ pulses were subtracted from B and D in Figure 1 (i.e., the C′ pulses are applied at the start of the delays denoted by B and D in Figure 1). The duration of $^{13}C^{\alpha}$ pulses and additional delays that affect $^{13}C'$ evolution were compensated by the addition/subtraction of the appropriate delays from the τ_d and τ'_d periods. In our implementation of the sequence the net time for cross-correlation is $T_C - 2{*}$pwco180, where pwco180 is the duration of the shaped $^{13}C'$ refocusing pulse (390 μs).

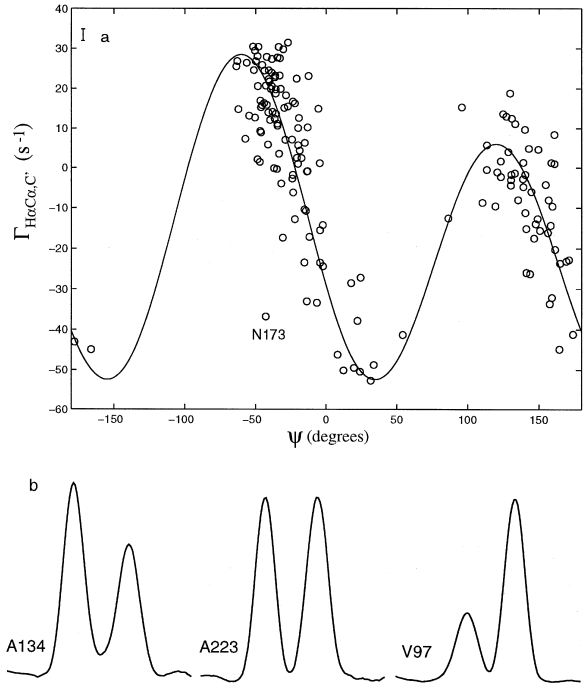

Figure 3. (a) Correlation between $\Gamma_{H\alpha C\alpha,C'}$ and ψ for non-glycine residues in a complex of β-cyclodextrin and maltose binding protein. A 1.4 mM sample, 20 mM sodium phosphate, 3 mM β-cyclodextrin, pH 7.2, was employed. A value of $T_C = 10.4$ ms was used with a data acquisition time of 110 h [$20 \times 26 \times 512$ complex points with acquisition times of 7.9, 21.4 and 64 ms in (t_1,t_2,t_3)]. Sensitivity enhancement was not used to record this data set. The data was processed using mirror-image linear prediction to double the time domain in each of t_1 and t_2, using the procedure outlined in Kay et al. (1991). (b) F_1 cross-sections through Ala 134, Ala 223 and Val 97, illustrating the range of $\Gamma_{H\alpha C\alpha,C'}$ values.

A comparison of Equations (2) and (8) indicates that because $\Gamma_{H\alpha C\alpha,C'}$ values are obtained from a ratio of two rather than four terms in the present method, the precision is higher than in our previous approach (Yang et al., 1997). Moreover, neglecting pulse imperfections, the sensitivity of the scheme of Figure 1 is predicted to be a factor of 2 higher than in our previous method. This can be understood by noting that the intensity of the cross peak at an ω_1 frequency of $\omega_{C'} - \pi J_{CH}$, $I_{2Q,\alpha+0Q,\beta}$, arises from both of the transitions $\alpha\beta\beta \rightarrow \alpha\alpha\alpha$ and $\beta\alpha\beta \rightarrow \beta\beta\alpha$ for the first half of the T_C period (A+B in Figure 1) and the corresponding transitions obtained after application of $^1H^\alpha$ and $^{13}C^\alpha$ 180° pulses during the second half. Thus, we can write

$$I_{2Q,\alpha+0Q,\beta}(T_C) = 2I_0\exp\{-0.5T_C(\Gamma_{2Q,\alpha} + \Gamma_{0Q,\beta})\} \quad (11.1)$$

In a similar fashion, recognizing that the cross peak at $\omega_{C'} + \pi J_{CH}$ derives from the transitions $\beta\beta\beta \rightarrow \beta\alpha\alpha(\alpha\alpha\beta \rightarrow \alpha\beta\alpha)$ and $\alpha\alpha\beta \rightarrow \alpha\beta\alpha(\beta\beta\beta \rightarrow \beta\alpha\alpha)$ for the first (second) half of the T_C period, the decay of $I_{2Q,\beta+0Q,\alpha}$ is given by

$$I_{2Q,\beta+0Q,\alpha}(T_C) = 2I_0\exp\{-0.5T_C(\Gamma_{2Q,\beta} + \Gamma_{0Q,\alpha})\} \quad (11.2)$$

In the case of our original experiment where zero- and double-quantum multiplet components are recorded (Yang et al., 1997),

$$[I_{2Q,\alpha}(T_C)I_{0Q,\beta}(T_C)]^{0.5} = I_0\exp\{-0.5T_C(\Gamma_{2Q,\alpha} + \Gamma_{0Q,\beta})\}$$
$$[I_{2Q,\beta}(T_C)I_{0Q,\alpha}(T_C)]^{0.5} = I_0\exp\{-0.5T_C(\Gamma_{2Q,\beta} + \Gamma_{0Q,\alpha})\} \quad (12)$$

A comparison of Equations (11) and (12) suggests, therefore, that the relative sensitivity of the two classes of experiments can be defined as $I_{2Q,\alpha+0Q,\beta}(T_C)/[I_{2Q,\alpha}(T_C)I_{0Q,\beta}(T_C)]^{0.5}$ (or $I_{2Q,\beta+0Q,\alpha}(T_C)/[I_{2Q,\beta}(T_C)I_{0Q,\alpha}(T_C)]^{0.5}$) and can be as large as a factor of 2. In practice the predicted sensitivity gain of 2 is not realized since the present experiment employs a larger number of pulses than the previous scheme in which intensities of each of the multiplet components in $^{13}C'$-$^{13}C^\alpha$ double- and zero-quantum spectra are recorded. In addition, recall that a selective $^{13}C^\alpha$ pulse is used in the center

of the constant time delay between points a and b in Figure 1, ensuring that refocusing of $^{13}C^{\alpha}$-$^{13}C^{\beta}$ couplings occurs in a manner which is independent of the delay chosen. In practice the selectivity is not perfect, decreasing the sensitivity of cross peaks arising from a number of residues. For a 2 ms RE-BURP pulse centered at 55 ppm, simulations establish that refocusing ($C^{\alpha}_{x,y} \rightarrow > 0.95C^{\alpha}_{x,y}$) extends from 63.3 to 46.7 ppm (500 MHz ^{1}H frequency). Thus, amino acids such as Val, Gly and Pro may not be completely refocused. In addition, inversion ($C^{\beta}_{z} \rightarrow < -0.95C^{\beta}_{z}$) extends over the same bandwidth so that magnetization from C^{β} of most Ser residues will be inverted, leading to sensitivity losses arising from $^{13}C^{\alpha}$-$^{13}C^{\beta}$ J-modulation. Simulations also indicate that $^{13}C^{\beta}$ carbons with chemical shifts less than 41.7 ppm or greater than 68.3 ppm are not affected by the application of the $^{13}C^{\alpha}$ selective pulse ($C^{\beta}_{z} \rightarrow > 0.93C^{\beta}_{z}$). Therefore, the sensitivity of correlations involving residues with downfield $^{13}C^{\beta}$ shifts ($>$ 41.7 ppm) may also be affected adversely. In the case of amino acids where the lack of selectivity of the refocusing pulse is an issue, the complete EXORCYCLE (Bodenhausen et al., 1977) of the $^{13}C^{\alpha}$ 180° selective pulse ensures that only the sensitivity of the measured correlations and not the accuracy of the measured cross-correlation relaxation rate is affected. This has been established both by calculations and by comparing measured $\Gamma_{H\alpha C\alpha,C'}$ values using the present method with results obtained previously (see below). Sensitivity gains of as much as a factor of 1.9 relative to our previous experiment are noted and for residues whose C^{α} shifts are refocused and whose C^{β} spins are not perturbed by the selective $^{13}C^{\alpha}$ refocusing pulse an average gain of a factor of 1.75 is measured.

Figure 2 illustrates a comparison of measured $\Gamma_{H\alpha C\alpha,C'}$ values obtained using the present method (○) and our previously published scheme (+) as a function of the backbone dihedral angle, Ψ, for the proteins ubiquitin (a) and CheY (b). The relations between $\Gamma_{H\alpha C\alpha,C'}$ and ψ obtained theoretically (Equations (9) and (10)) assuming standard bond lengths and angles and values for the orientation and principal components of the $^{13}C'$ chemical shift tensor described in Teng et al. (1992), are given by the solid curves in the figure. Average errors in $\Gamma_{H\alpha C\alpha,C'}$ values have decreased by a factor of approximately 2, the result of the improved sensitivity and the fact that a ratio of only two rather than four experimentally derived intensities is required in the calculation of the cross-correlation rate (see Equations (2) and (8)). In the case of ubiquitin (CheY), $\Gamma_{H\alpha C\alpha,C'}$ values for 63 (87) and 60 (82) non-glycine residues were obtained from data sets recorded with our previous method (Yang et al., 1997) and the present scheme, respectively. The imperfect selectivity of the $^{13}C^{\alpha}$ refocusing pulse (see above) results in only a small decrease in the numbers of cross peaks observed in spectra of both of these proteins; correlations for only two residues in ubiquitin (Leu 67 and 69) and three residues in CheY (Leu 9, Ser 58 and Leu 84) were not observed in the new experiment. The remaining differences in the numbers of correlations observed result from different patterns of spectral overlap observed in the two classes of experiments.

Figure 3a shows the $\Gamma_{H\alpha C\alpha,C'}$ versus ψ profile from an application to a complex of β-cyclodextrin and maltose binding protein (42 kDa). Cross-sections (F_1) through correlations from residues Ala 134, Ala 223 and Val 97 are illustrated in Figure 3b to indicate that very different cross-correlation relaxation rates (magnitude and sign) can be obtained. Because of the large size of the complex and the concomitant large values for both auto- and cross-correlation relaxation rates a T_C (A + B + C + D) delay of 10.4 ms ($< 1/J_{CC}$) was chosen and rates for 159 residues were obtained. The lack of data for approximately half of the residues in the complex reflects to a large extent resolution limitations, imposed by the necessarily short t_1 acquisition time and the 370 residues in the molecule! In addition, cross peaks from a number of residue types are of low intensity or are missing due to the bandwidth of the selective $^{13}C^{\alpha}$ refocusing pulse applied in the center of the carbon evolution period (see above). It is noteworthy that the sensitivity of our previous scheme for measuring $\Gamma_{H\alpha C\alpha,C'}$ is not sufficient for measurements on molecules of this size.

On average, reasonable agreement between measured $\Gamma_{H\alpha C\alpha,C'}$ rates and predicted values based on Equations (8)–(10) and ψ values derived from the X-ray structure of the complex (Sharff et al., 1993) are noted. A number of outliers are observed, however. In particular, measured rates for some of the residues with ψ values in the β-sheet region of (ϕ,ψ) space are larger than predicted, assuming a global overall correlation time of 17.2 ± 0.8 ns, determined by ^{15}N relaxation measurements (Farrow et al., 1994). Interestingly, many of the outlying residues cluster in the region Leu 262–Asn 267 and are part of a β-strand extending between the two domains of the molecule. In the absence of additional structural information, the

$\Gamma_{H\alpha C\alpha,C'}$ values measured for these residues would place their ψ values in regions which are inconsistent with values for the dihedral angle derived from the X-ray structure. This emphasizes the importance of using a combination of cross-correlation rates with chemical shifts to ensure that accurate ψ values are obtained. In this regard, inspection of $(\Delta C^{\alpha} - \Delta C^{\beta})_{smoothed}$ versus residue (where Δ refers to the difference between measured and random coil chemical shift values) (Metzler et al., 1993) shows that the region extending from Lys 256 to Val 261 and from Ser 263 to Gly 266 has secondary shifts that are consistent with β-strand secondary structure. It is noteworthy that even in the limit of perfect data the multi-valued nature of the $\Gamma_{H\alpha C\alpha,C'}$ versus ψ surface dictates that additional information, such as $^{13}C^{\alpha}$ and $^{13}C^{\beta}$ chemical shifts, is necessary in order to assign a value of ψ to a particular residue. Finally, the largest outlying residue is Asn 173, for which predicted and measured $\Gamma_{H\alpha C\alpha,C'}$ values of approximately $+21.5$ and -37 are observed. It is interesting that this residue has the highest temperature factors in the molecule (57 $Å^2$ at the C^{α} position) and the discrepancy may well reflect problems with the X-ray structure.

In summary, we have described a new pulse scheme for measuring interference between $^{13}C^{\alpha}$-$^{1}H^{\alpha}$ dipolar and $^{13}C'$ CSA relaxation mechanisms, providing a straightforward approach for measuring the backbone dihedral angle ψ. The method offers a number of significant advantages over our previously published experiment, especially improved sensitivity. The utility of the method for applications to high-molecular-weight proteins is demonstrated with results obtained on a 42 kDa complex of β-cyclodextrin and maltose binding protein.

Acknowledgements

The authors are grateful to Professors J. Wand (SUNY, Buffalo) and Rick Dahlquist (University of Oregon) for kindly supplying the ^{15}N,^{13}C-labeled samples of ubiquitin and CheY used in this study, to Professor Kalle Gehring (McGill University) for providing the maltose binding protein plasmid, and to Mr. Randall Willis (Hospital for Sick Children) for preparation of the maltose binding protein sample. This research was supported by the Medical Research Council of Canada. L.E.K. is an International Howard Hughes Research Scholar. K.H.G. was supported by a postdoctoral fellowship from the Helen Hey Whitney Foundation.

References

Abragam, A. (1961) *Principles of Nuclear Magnetism*, Clarendon Press, Oxford, p. 289.

Bax, A., Griffey, R.H. and Hawkings, B.L. (1983) *J. Magn. Reson.*, **55**, 301–315.

Bax, A. and Ikura, M. (1991) *J. Biomol. NMR*, **1**, 99–104.

Bodenhausen, G., Freeman, R. and Turner, D.L. (1977) *J. Magn. Reson.*, **27**, 511–514.

Delaglio, F., Grzesiek, S., Vuister, G.W., Zhu, G., Pfeifer, J. and Bax, A. (1995) *J. Biomol. NMR*, **6**, 277–293.

Farrow, N.A., Muhandiram, R., Singer, A.U., Pascal, S.M., Kay, C.M., Gish, G., Shoelson, S.E., Pawson, T., Forman-Kay, J.D. and Kay, L.E. (1994) *Biochemistry*, **33**, 5984–6003.

Garrett, D.S., Powers, R., Gronenborn, A.M. and Clore, G.M. (1991) *J. Magn. Reson.*, **95**, 214–220.

Geen, H. and Freeman, R. (1991) *J. Magn. Reson.*, **93**, 93–141.

Goldman, M. (1984) *J. Magn. Reson.*, **60**, 437–452.

Kay, L.E. (1993) *J. Am. Chem. Soc.*, **115**, 2055–2056.

Kay, L.E., Ikura, M., Tschudin, R. and Bax, A. (1990) *J. Magn. Reson.*, **89**, 496–514.

Kay, L.E., Ikura, M., Zhu, G. and Bax, A. (1991) *J. Magn. Reson.*, **91**, 422–428.

Kay, L.E., Keifer, P. and Saarinen, T. (1992) *J. Am. Chem. Soc.*, **114**, 10663–10665.

Kupce, E., Boyd, J. and Campbell, I.D. (1995) *J. Magn. Reson.*, **B106**, 300–303.

Marion, D., Ikura, M., Tschudin, R. and Bax, A. (1989) *J. Magn. Reson.*, **85**, 393–399.

McCoy, M. and Mueller, L. (1992) *J. Am. Chem. Soc.*, **114**, 2108–2110.

Metzler, W.J., Constantine, K.L., Friedrichs, M.S., Bell, A.J., Ernst, E.G., Lavoie, T.B. and Mueller, L. (1993) *Biochemistry*, **32**, 13818–13829.

Mueller, L. (1979) *J. Am. Chem. Soc.*, **101**, 4481–4484.

Reif, B., Hennig, M. and Griesinger, C. (1997) *Science*, **276**, 1230–1233.

Schleucher, J., Sattler, M. and Griesinger, C. (1993) *Angew. Chem. Int. Ed. Engl.*, **32**, 1489–1491.

Shaka, A.J., Keeler, J., Frenkiel, T. and Freeman, R. (1983) *J. Magn. Reson.*, **52**, 335–338.

Sharff, A.J., Rodseth, L.E. and Quiocho, F.A. (1993) *Biochemistry*, **32**, 10553–10559.

Stock, A.M., Martinez-Hackert, E., Rasmussen, B.F., West, A.H., Stock, J.B., Ringe, D. and Petsko, G.A. (1994) *Biochemistry*, **32**, 13375–13380.

Teng, Q., Iqbal, M. and Cross, T.A. (1992) *J. Am. Chem. Soc.*, **114**, 5312–5321.

Vijay-Kumar, S., Bugg, C.E. and Cook, W.J. (1987) *J. Mol. Biol.*, **194**, 531–544.

Vuister, G.W. and Bax, A. (1992) *J. Magn. Reson.*, **98**, 428–435.

Werbelow, L.G. and Grant, D.M. (1977) *Adv. Magn. Reson.*, **9**, 189–299.

Yang, D., Konrat, R. and Kay, L.E. (1997) *J. Am. Chem. Soc.*, **119**, 11938–11940.